On the Design of Target Beampatterns for Differential Microphone Arrays

Chao Pan, Jingdong Chen, Jacob Benesty, and Guangming Shi

***Abstract*—Differential microphone arrays (DMAs) have many interesting properties and have been widely used in acoustic, audio, and speech applications. A critical part of a DMA is the differential beamformer, which is generally designed in two important steps: 1) specifying a target beampattern based on what differential sound pressure field the DMA is expected to respond to and 2) designing the differential beamforming filter so that the resulting beampattern matches the target one. Most efforts in the study of DMAs so far have focused on the second step while choosing one of the limited patterns available in the literature as the target beampattern. Since it governs how the array performs, how to design the target beampattern is an important problem, which this paper addresses. The major contributions of this paper consists of the following four aspects. First, a positive superposition theorem is presented, which shows that the linear combination of effective beampatterns with non-negative coefficients is always an effective beampattern. Second, we propose a general approach to the design of target DMA beampatterns based on the positive superposition theorem. Third, an overview of the classical target beampatterns is provided and discussion is made on how to form effective base patterns. Fourth, we show that the smallest first null of a DMA is $\pi/(2N)$ with N being the DMA order, which provides the rule of setting nulls in practice. Finally, with examples, we show that with the use of the alternating-direction-method-of-multipliers algorithm, the proposed approach is able to generate useful DMA target beampatterns.**

***Index Terms*—Differential microphone arrays, differential beamforming, target beampattern, ADMM algorithm.**

Manuscript received July 18, 2018; revised January 6, 2019 and April 8, 2019; accepted May 7, 2019. Date of publication May 20, 2019; date of current version May 31, 2019. This work was supported in part by the Fundamental Research Funds for the Central Universities (FRFCU) (No. 20101196782), in part by the National Natural Science Foundation of China (NSFC) (Nos. 61632019, 61836008, 61572387, 61871304, 61672404), in part by the Foundation for Innovative Research Groups of NSFC (No. 61621005), and in part by the FRFCU (No. JB181702). The work of J. Chen was supported in part by the NSFC key program (No. 61831019), in part by the NSFC–ISF joint research program (No. 61761146001), and in part by the NSFC Distinguished Young Scientists Fund (No. 61425005). The associate editor coordinating the review of this manuscript and approving it for publication was Dr. Andy W. H. Khong. *(Corresponding author: Chao Pan.)*

C. Pan is with the Optoelectronic Imaging and Brain-inspired Perception Laboratory, School of Artificial Intelligence, Xidian University, Xi'an 710071, China, and also with the Center of Intelligent Acoustics and Immersive Communications, Northwestern Polytechnical University, Xi'an 710072, China (e-mail: chaopan@xidian.edu.cn).

J. Chen is with the Center of Intelligent Acoustics and Immersive Communications, Northwestern Polytechnical University, Xi'an 710072, China (e-mail: jingdongchen@ieee.org).

J. Benesty is with the INRS-EMT, University of Quebec, Montreal, QC H5A 1K6, Canada (e-mail: benesty@emt.inrs.ca).

G. Shi is with the Optoelectronic Imaging and Brain-Inspired Perception Laboratory, School of Artificial Intelligence, Xidian University, Xi'an 710071, China (e-mail: gmshi@xidian.edu.cn).

Digital Object Identifier 10.1109/TASLP.2019.2918081

I. Introduction

UNLIKE traditional microphone arrays that are responsive to the sound pressure field, differential microphone arrays (DMAs) estimate the signal of interest while rejecting noise simultaneously by measuring the differential sound pressure field. DMAs have a number of salient properties including: 1) their aperture is generally small because the inter-element spacing of the array is required to be small to measure the differential sound pressure field; 2) the beampatterns of DMAs are approximately independent of frequencies [1]–[3]; 3) the directivity factors of DMAs are usually higher than those of additive microphone arrays with the same number of senors. These features make DMAs attractive in communication and human-machine interface systems in order to acquire and process broadband speech and audio signals in room acoustic environments. As a result, intensive efforts have been devoted to the design of DMAs and development of the associated beamforming algorithms.

The basic principle of DMAs can be traced back to the 1940s when Olson demonstrated that measuring the 1st-order differential sound pressure field can make a differential sensor have some spatial directivity [1]. This principle was then used to design DMAs and it was reported that different directivity patterns can be achieved by either applying proper time delays to the signals before subtraction or combing different orders of DMAs. Later in [3]–[5], Elko *et al.* systematically investigated DMAs based on a multistage-subtraction (multistage-cascaded) structure. The relationship between the time delays at each stage and the corresponding directivity pattern were investigated and some classical beampatterns such as the dipole, cardioid, supercardioid, and hypercardioid were derived. In [2], [6], and [7], a null-constrained DMA design method was proposed, and the sensitivity of DMAs to the array imperfections were studied systematically. Meanwhile, the so-called robust DMAs, which have higher white noise gain (WNG) as compared to the traditional DMAs, were proposed by sacrificing the order of DMAs and exploiting the remaining degrees of freedom from the array to improve WNG. In [2], [8]–[10], series-expansion methods were proposed to design differential beamformers, which share the same principle as the traditional series-expansion-based beamforming approaches [11]–[17]. Besides the aforementioned works, other interesting contributions have been made over the last few decades, e.g., study of DMA performance in the presence of different types of noise [18], [19], and design of DMAs with different array geometries [20]–[22].

Early efforts in DMA research was focused on DMA principles, and the design of the array and the associated circuits. As digital signal processing becomes more dominant, the focus of DMA design has slowly shifted from the array design to the design of differential beamformers, which are the central component of a DMA. Generally, the design of differential beamformers consists of two important steps. The first one is to specify a target beampattern based on the application requirements including what differential sound pressure field the DMA is expected to respond to, what directivity factor and WNG the DMA is required to achieve, etc. While the second step is to design the differential beamforming filter so that the resulting beampattern matches the target beampattern as much as possible. So far, most efforts in the literature are devoted to the second step while choosing a very limited number of patterns available in the literature as the target beampattern, e.g., the dipole which has a grating lobe at the opposite look direction [2], [5], the cardioid which has a higher WNG than other beampatterns [23], the hypercardioid which has the maximum array gain in the spherical/cylindrical isotropic noise [5], [24], the supercardioid which has the maximum (weighted) front-to-back ratio [5], [24], the patterns with a flat response in some region [25], and the patterns derived from the Chebyshev polynomials [5]. Since it governs how the array performs in terms of the array gain, robustness, and directional noise suppression, how to design the target beampattern is an important problem, which will be addressed in this paper. There are two important factors that have to be considered during the design of a target beampattern.

1) *Effectiveness*: it means that the maximum gain of the beampattern has to occur in the look direction; otherwise, the resulting differential beamformer may either attenuate the signal of interest from the look direction or amplifies noise from other directions.
2) *Requirements of the Applications*: the target beampattern should have nulls in the directions where strong noise and interferences occur most likely in the application. In other words, the target beampattern should achieve maximum noise rejection while preserving the signal of interest.

These two factors will be jointly considered in this paper. We propose a general approach to the design of target beampatterns based on a positive superposition theorem. With this approach, a target beampattern is expressed as a linear combination of a set of base patterns with nonnegative weighting coefficients, and its effectiveness is guaranteed by the positive superposition theorem. Using this method, we formulate the target beampattern design problem into an optimization one. We then show how to solve this optimization problem with the alternating-direction-method-of-multipliers (ADMM) algorithm [26]. Since the presented approach requires a set of effective base patterns, we derive several classes which are based on some classical patterns developed in the literature. Examples are presented to validate the feasibility of the presented method.

The organization of the rest of this paper is as follows. Section II presents the background and motivation of this work as well as a new design approach. Section III discusses how to design effective target beampatterns with the proposed approach based on the null information, and how to solve the optimization problem with the ADMM algorithm. The construction of base patterns for the presented approach is addressed in Section IV. Section V verifies the feasibility of developed method with examples. Finally, conclusions are summarized in Section VI.

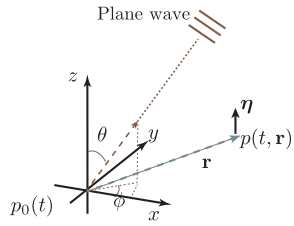

Fig. 1. Illustration of the used DMA coordinate system.

II. Background, Objective, and Approach

A. Background Knowledge and Target Beampatterns of DMAs

Let us denote the sound pressure at the original point (0, 0, 0) as $p_0(t)$, where t is the time index. If we consider a plane wave propagating to the position $\mathbf{r} \triangleq [r_x \ r_y \ r_z]^T$, with the superscript ^{T} being the transpose operator, from the direction (θ, ϕ) as illustrated in Fig. 1 and neglect the propagation loss, the sound pressure at $\mathbf{r}$ can be expressed as

$$p(t, \mathbf{r}) = p_0(t - \tau_{\mathbf{r}}), \tag{1}$$

where

$$\tau_{\mathbf{r}} = -\frac{1}{c}\left(r_x \sin\theta\cos\phi + r_y \sin\theta\sin\phi + r_z\cos\theta\right), \tag{2}$$

with c being the sound speed in the air.

The first-order differential sound pressure field is defined by the directional derivative of $p(t, \mathbf{r})$ along a direction $\boldsymbol{\eta} \triangleq [\eta_x \ \eta_y \ \eta_z]^T$. Mathematically, the first-order differential sound pressure field can be expressed as

$$\mathbb{D}_{\boldsymbol{\eta}}^{(1)}\left[p(t, \mathbf{r})\right] \triangleq \lim_{\mu\to 0}\frac{p(t, \mu\boldsymbol{\eta} + \mathbf{r}) - p(t, \mathbf{r})}{\mu} \tag{3}$$

$$= \frac{\partial p(t, \mathbf{r})}{\partial r_x}\eta_x + \frac{\partial p(t, \mathbf{r})}{\partial r_y}\eta_y + \frac{\partial p(t, \mathbf{r})}{\partial r_z}\eta_z. \tag{4}$$

Now, let us consider a particular case where $\eta_x = \eta_y = 0$ and $\eta_z = 1$, i.e., the direction of the derivative is along the z-axis. In this case, (4) can be rewritten as

$$\begin{aligned}\mathbb{D}_{\boldsymbol{\eta}}^{(1)}\left[p(t, \mathbf{r})\right] &= \frac{\partial p(t, \mathbf{r})}{\partial r_z} \\ &= \mathcal{F}^{-1}\left[\frac{\partial P(\omega, \mathbf{r})}{\partial r_z}\right] \\ &= \mathcal{F}^{-1}\left[(\jmath\omega/c)\cos\theta P(\omega, \mathbf{r})\right] \\ &= \cos\theta \times \mathcal{F}^{-1}\left[(\jmath\omega/c)\, P(\omega, \mathbf{r})\right],\end{aligned} \tag{5}$$

where $P(\omega, \mathbf{r}) = \mathcal{F}\left[p(t, \mathbf{r})\right]$ and $\jmath$ is the imaginary unit, with $\mathcal{F}\left[\cdot\right]$ being the Fourier transform and $\mathcal{F}^{-1}\left[\cdot\right]$ its inverse.

In a similar way, the n th-order differential sound pressure field along the z-axis can be derived as

$$\begin{aligned}\mathbb{D}_{\boldsymbol{\eta}}^{(n)}\left[p(t,\mathbf{r})\right] &= \frac{\partial^n p(t,\mathbf{r})}{\partial r_z^n}\\ &= \mathcal{F}^{-1}\left[\frac{\partial^n P(\omega,\mathbf{r})}{\partial r_z^n}\right]\\ &= \mathcal{F}^{-1}\left[(\jmath\omega/c)^n\cos^n(\theta)P(\omega,\mathbf{r})\right]\\ &= \cos^n(\theta)\times\mathcal{F}^{-1}\left[(\jmath\omega/c)^n P(\omega,\mathbf{r})\right]\\ &= \cos^n(\theta)\times\left[p(t,\mathbf{r})*\hbar(t)\right], \end{aligned} \tag{6}$$

where $\hbar(t)=\mathcal{F}^{-1}\left[(\jmath\omega/c)^n\right]$ and $*$ denotes linear convolution. Therefore, by measuring the differential sound pressure field, a system can attenuate plane waves from different directions in a different manner. This naturally produces a spatial directivity pattern, which is also referred to as the *beampattern* in array signal processing. As seen, the beampattern associated with the N th-order differential sound pressure field is $\cos^N(\theta)$, which is the well-known dipole pattern. However, this directivity pattern may not be appropriate or optimal for many if not most applications.

To increase the diversity of the beampatterns, a popular way is to measure a combination of differential sound pressure fields from the order 0 to the order N, instead of just the N th-order one. According to (6), the corresponding beampatterns can then be expressed as

$$\mathcal{B}(\theta)=\sum_{n=0}^{N}\varrho_n\cos^n(\theta), \tag{7}$$

where ϱ_n's are some real coefficients, N is a nonnegative integer number, and $\cos^n(\theta)$ is the beampattern associated with the nth order differential sound pressure field. For linear DMAs, it is generally assumed that the look direction is at the endfire direction, i.e., $\theta=0^\circ$. Therefore, the sum of the coefficients ϱ_n's should satisfy

$$\sum_{n=0}^{N}\varrho_n=1. \tag{8}$$

While it gives a great diversity in the beampatterns, (7) also brings some challenges, e.g., if the values of the coefficients ϱ_n's are not properly set, the resulting beampattern may attenuate the signal of interest from the look direction while amplifying noise from other directions.

Now, given a small spacing microphone array that can perform differential beamforming, the design of differential beamformers generally follows two steps: 1) choose a target DMA beampattern by setting proper values of ϱ_n's in (7); and 2) design the differential beamforming filter so that the resulting beampattern is as close as possible to the target beampattern. In the literature, most efforts focused on the second step while typically choosing the dipole, cardioid, supercardioid, or hypercardioid patterns as the target beampatterns. In this paper, we focus on the first step and present a general approach to the design of target beampatterns. For ease of exposition, we focus on linear DMAs and assume that the look direction is 0°. It should be noted that the method and results presented in this work can be easily generalized to other array geometries with different look directions.

B. Sufficient Condition for Effective Target Beampatterns

Definititon II.1 (SE-condition): A target beampattern is an effective and a valid one if and only if the maximum of its amplitude appears at the look direction. Otherwise, the associated DMA will either attenuate the signal of interest from the look direction or amplify noise from some other directions. So, the sufficient condition for a pattern to be an effective target beampattern is expressed as

$$\left|\mathcal{B}(\theta)\right|\le\left|\mathcal{B}(0^\circ)\right|,\ \forall\theta\in[0^\circ,180^\circ]. \tag{9}$$

To ensure that the signal of interest from the look direction is not distorted, it is desirable to have the following constraint:

$$\mathcal{B}(0^\circ)=1. \tag{10}$$

For convenience, we define the condition in (9) and (10) as the *SE-condition*, where "SE" stands for "sufficient condition for a target beampattern to be effective."

C. Properties of the Desired Target Beampattern

According to (7), $\mathcal{B}(\theta)$ is an N th-order polynomial with respect to $\cos\theta$. Therefore, it can be rewritten as [2]

$$\mathcal{B}(\theta)=\zeta_0\prod_{n=1}^{N}\left(\cos\theta-\zeta_n\right), \tag{11}$$

where $\zeta_n=\cos\theta_{0;n}$ with $\theta_{0;n}$ $(n=1,2,\ldots,N)$ being the nulls of the beampattern, and $\zeta_0=1/\prod_{n=1}^{N}(1-\zeta_n)$ according to (10).

For a given set of the nulls, it is clear that the beampattern can be determined according to (11). In case that the resulting beampattern satisfy the SE-condition, the set of the nulls is called *well-conditioned*; otherwise, it is called *ill-conditioned*.

The objective of this paper is to find approaches to the design of target beampatterns based on a set of nulls, which satisfy the SE-condition.

D. Proposed Approach to Effective Target Beampatterns

Theorem II.1 (Positive Superposition Theorem): For a set of beampatterns $\{\mathcal{B}_l(\theta),\ l=0,1,2,\ldots,L\}$ of no more than the Nth order satisfying the SE-condition and the distortionless constraint in (10), and a set of nonnegative coefficients $\{\alpha_l,\ l=0,1,2,\ldots,L\}$, the following beampattern:

$$\mathcal{B}_{\boldsymbol{\alpha}}(\theta)=\sum_{l=0}^{L}\alpha_l\mathcal{B}_l(\theta), \tag{12}$$

where

$$\boldsymbol{\alpha}=\left[\alpha_0\ \ \alpha_1\ \ \cdots\ \ \alpha_L\right]^T, \tag{13}$$

always satisfies the SE-condition, i.e., the beampattern given in (12) is also effective and valid.

Proof: Consider the Holder's inequality:

$$\left(\sum_i |a_i b_i|\right) \le \left(\sum_i |a_i|^p\right)^{1/p} \left(\sum_i |b_i|^q\right)^{1/q}, \quad (14)$$

where $1/p + 1/q = 1, \forall p, q \in [1, \infty]$. For $p = 1$ and $q = \infty$, we have

$$\left(\sum_i |a_i b_i|\right) \le \left(\sum_i |a_i|\right) \max_i |b_i|. \quad (15)$$

Given that $(\sum_i a_i b_i)^2 \le (\sum_i |a_i b_i|)^2$, we have

$$\left(\sum_i a_i b_i\right)^2 \le \left(\sum_i |a_i|\right)^2 \left(\max_i |b_i|\right)^2. \quad (16)$$

Setting $a_i = \alpha_i$ and $b_i = \mathcal{B}_i(\theta)$, and considering that $\alpha_i \ge 0$ and $\max_i |\mathcal{B}_i(\theta)| \le 1$, we have

$$\begin{aligned}\left[\sum_i \alpha_i \mathcal{B}_i(\theta)\right]^2 &\le \left[\sum_i |\alpha_i|\right]^2 \left[\max_i |\mathcal{B}_i(\theta)|\right]^2 \\ &\le \left(\sum_i \alpha_i\right)^2. \end{aligned} \quad (17)$$

It follows immediately then that

$$\begin{aligned}\mathcal{B}^2_{\boldsymbol{\alpha}}(\theta) &= \left[\sum_l \alpha_l \mathcal{B}_l(\theta)\right]^2 \\ &\le \left(\sum_l \alpha_l\right)^2 = \mathcal{B}^2_{\boldsymbol{\alpha}}(0). \end{aligned} \quad (18)$$

End of the proof. ■

As long as the beampattern is formed based on the positive superposition theorem, the effectiveness is guaranteed theoretically. According to (12), the design of a target beampattern consists of two steps.

- Identify a set of effective beampatterns, i.e., $\mathcal{B}_l(\theta),\ l = 0, 1, \ldots, L$, which satisfy the SE-condition.
- Find a set of nonnegative coefficients, i.e., α_l's, so that the beampattern formed according to (12) have nulls at the desired null directions $\theta_{0;n}$ $(n = 1, 2, \ldots, N)$.

The set of effective beampatterns can be formed by the widely used beampatterns including cardioid, supercardioid, hypercardioid, etc, details of which will be presented in Section IV. In Section III, we show how to transform the determination of the values of α_l's into an optimization problem and how to solve it using the well-known ADMM algorithm.

III. Target Beampattern Design With the Null Information

Suppose that we have $L + 1$ effective beampatterns $\mathcal{B}_l(\theta)$, $l = 0, 1, \ldots, L$ of orders no more than N. Now, designing a target beampattern becomes one of finding a proper set of nonnegative α_l's such that the beampattern $\mathcal{B}_{\boldsymbol{\alpha}}(\theta)$ has nulls in the desired null directions. For convenience, we call $\mathcal{B}_l(\theta)$'s the *base patterns* in the rest of this paper.

Since they are polynomials with respect to $\cos\theta$ of orders no more than N, all the base patterns can be expressed as

$$\mathcal{B}_l(\theta) = \mathbf{x}^T(\theta)\boldsymbol{\varrho}_l,\ \forall l = 0, 1, \ldots, L, \quad (19)$$

where

$$\mathbf{x}(\theta) = \left[1\ \cos\theta\ \cdots\ \cos^N\theta\right]^T, \quad (20)$$

$$\boldsymbol{\varrho}_l = \left[\varrho_{l;0}\ \varrho_{l;1}\ \cdots\ \varrho_{l;N}\right]^T. \quad (21)$$

Substituting (19) into (12), we can rewrite the beampattern as

$$\begin{aligned}\mathcal{B}_{\boldsymbol{\alpha}}(\theta) &= \sum_{l=0}^{L} \alpha_l \mathbf{x}^T(\theta)\boldsymbol{\varrho}_l \quad (22)\\ &= \mathbf{x}^T(\theta)\boldsymbol{\Psi}\boldsymbol{\alpha}, \quad (23)\end{aligned}$$

where

$$\boldsymbol{\Psi} = \left[\boldsymbol{\varrho}_0\ \boldsymbol{\varrho}_1\ \cdots\ \boldsymbol{\varrho}_L\right]. \quad (24)$$

If we assume that the N desired nulls are in the directions $\theta_{0;1}, \theta_{0;2}, \ldots, \theta_{0;N}$, the optimization problem of finding the vector $\boldsymbol{\alpha}$ can be described as

$$\begin{aligned}\mathcal{B}_{\boldsymbol{\alpha}}(\theta_{0;n}) = 0,\ \ &\forall n = 1, 2, \ldots, N \\ \text{s.t.}\ \ &\mathbf{x}^T(0)\boldsymbol{\Psi}\boldsymbol{\alpha} = 1 \\ &\alpha_l \ge 0,\ \forall l = 0, 1, \ldots, L, \end{aligned} \quad (25)$$

where the equality constraint ensures that the array response in the look direction is 1, and the inequality constraints ensure the effectiveness of the resulting target beampattern.

Unfortunately, the optimization problem in (25) does not have a feasible solution in general. Let us relax the problem as follows:

$$\begin{aligned}\min_{\boldsymbol{\alpha}} \sum_{n=1}^{N} |\mathcal{B}_{\boldsymbol{\alpha}}(\theta_{0;n})| \quad &\text{s.t. } \mathbf{x}^T(0)\boldsymbol{\Psi}\boldsymbol{\alpha} = 1 \\ &\alpha_l \ge 0,\ \forall l = 0, 1, \ldots, L. \end{aligned} \quad (26)$$

Here, we choose the sum of the absolute values instead of the squared absolute values as the cost function. The underlying reason is that the ℓ_1-norm leads to sparse solutions [27], and a sparser solution in our case means more nulls in the beampattern (an example is shown in Fig. 2).

Substituting (23) into (26), we can rewrite the optimization problem as

$$\begin{aligned}\min_{\boldsymbol{\alpha}} \|\mathbf{X}^T\boldsymbol{\Psi}\boldsymbol{\alpha}\|_1 \quad &\text{s.t. } \mathbf{x}^T(0)\boldsymbol{\Psi}\boldsymbol{\alpha} = 1 \\ &\alpha_l \ge 0,\ \forall l = 0, 1, \ldots, L, \end{aligned} \quad (27)$$

where $\|\cdot\|_1$ denotes the ℓ_1-norm of a vector and

$$\mathbf{X} = \left[\mathbf{x}(\theta_{0;1})\ \mathbf{x}(\theta_{0;2})\ \cdots\ \mathbf{x}(\theta_{0;N})\right] \quad (28)$$

is a matrix of size $(N + 1) \times N$. It can be verified that the term $\mathbf{x}^T(0)\boldsymbol{\Psi}$ is actually an all-one vector due to the constraint in (10). This optimization problem is now convex. Various methods can be applied to find the optimal solution. In this work, we solve the problem in (27) using the well-known ADMM algorithm [26]; details of which are shown in Appendix A. The interested reader can also use some existing toolboxes such as CVX [28]. Note

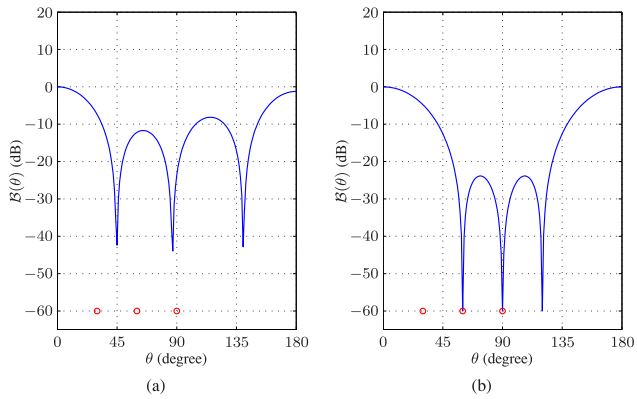

Fig. 2. Beampatterns resulting from (a) minimization of the sum of the squared absolute values and (b) minimization of the sum of the absolute values. The order of the beampattern is $N = 3$ and the set of the desired nulls is $\{30^\circ, 60^\circ, 90^\circ\}$.

that discussing the ADMM algorithm is not the main thrust of this paper.

IV. Examples of Base Patterns

In this section, we discuss base patterns of order Q ($Q \leq N$) based on the classical target beampatterns including the dipole, cardioid, supercardioid, hypercardioid, Chebyshev beampatterns, etc.

A. Null Constrained

Suppose that the nulls of the base pattern of order Q are known *a priori*. We have

$$\mathcal{B}(\theta) = \frac{1}{\prod_{q=1}^{Q}(1-\zeta_q)} \prod_{q=1}^{Q} (\cos\theta - \zeta_q), \tag{29}$$

where $\zeta_q = \cos\theta_{0;q}$ $(q = 1, 2, \ldots, Q)$ with $\theta_{0;q}$'s being the nulls of the beampattern.

In the case that all the nulls are in $[90^\circ, 180^\circ]$, we have $\zeta_q \in [-1, 0],\ \forall q = 1, 2, \ldots, Q$. It can be proved that

$$|\cos\theta - \zeta_q|^2 \leq |1 - \zeta_q|^2,\ \forall q = 1, 2, \ldots, Q. \tag{30}$$

Thus, we have

$$\prod_{q=1}^{Q} |\cos\theta - \zeta_q|^2 \leq \prod_{q=1}^{Q} |1 - \zeta_q|^2, \tag{31}$$

which leads to

$$\mathcal{B}^2(\theta) \leq \mathcal{B}^2(0). \tag{32}$$

Therefore, we conclude that the base pattern with all the nulls in $[90^\circ, 180^\circ]$ always satisfies the SE-condition.

Let us consider a particular case where all the nulls of the base pattern are in the same direction [23], i.e.,

$$\begin{aligned}\mathcal{B}(\theta) &= \frac{1}{(1-\zeta_1)^Q}(\cos\theta - \zeta_1)^Q \\ &= \sum_{q=0}^{Q} \frac{Q!}{(Q-q)!q!} \times \frac{(-\zeta_1)^{Q-q}}{(1-\zeta_1)^Q} \cos^q\theta,\end{aligned} \tag{33}$$

where $\zeta_1 = \cos\theta_{0;1} \in [-1, 0]$, with $\theta_{0;1}$ being the unique null of multiplicity of Q. In this particular case, we have

$$\varrho_q = \begin{cases} \dfrac{Q!}{(Q-q)!q!} \times \dfrac{(-\zeta_1)^{Q-q}}{(1-\zeta_1)^Q}, & q \leq Q \\ 0, & \text{else} \end{cases}. \tag{34}$$

Setting Q and ζ_1 to different values, we can generate many base patterns. One can check that the well-known dipole and cardioid patterns of order Q ([2], [5]) correspond to $\zeta_1 = 0$ and $\zeta_1 = -1$ in (33), respectively.

B. Hypercardioid

The hypercardioid corresponds to the beampattern with maximum directivity factor (DF). Its coefficients can be derived from [5], [24]

$$\begin{aligned}\boldsymbol{\varrho}_{\mathrm{Hd}} &= \arg\max_{\boldsymbol{\varrho}} \frac{\mathcal{B}^2(0)}{\frac{1}{2}\int_0^\pi \mathcal{B}^2(\theta)\sin\theta d\theta} \text{ s.t. } \boldsymbol{\varrho}^T\mathbf{x}(0) = 1 \\ &= \arg\min_{\boldsymbol{\varrho}} \boldsymbol{\varrho}^T\boldsymbol{\Upsilon}_{\mathrm{Hd}}\boldsymbol{\varrho} \text{ s.t. } \boldsymbol{\varrho}^T\mathbf{x}(0) = 1 \\ &= \frac{\boldsymbol{\Upsilon}_{\mathrm{Hd}}^{-1}\mathbf{x}(0)}{\mathbf{x}^T(0)\boldsymbol{\Upsilon}_{\mathrm{Hd}}^{-1}\mathbf{x}(0)},\end{aligned} \tag{35}$$

where $\boldsymbol{\Upsilon}_{\mathrm{Hd}}$ is a matrix of size $(Q+1) \times (Q+1)$ whose (i, j)th element is

$$[\boldsymbol{\Upsilon}_{\mathrm{Hd}}]_{i,j} = \frac{1}{2}\int_{-1}^{1} x^{i+j-2}dx = \frac{1 + (-1)^{i+j}}{2(i+j-1)}. \tag{36}$$

Note that a more general case of the hypercardioid can be derived from [24]

$$\max_{\boldsymbol{\varrho}} \frac{\mathcal{B}^2(0)}{\frac{1}{2}\int_0^\pi \psi(\theta)\mathcal{B}^2(\theta)\sin\theta d\theta} \text{ s.t. } \boldsymbol{\varrho}^T\mathbf{x}(0) = 1, \tag{37}$$

where $\psi(\theta)$ is a proper weight function. For example, if $\psi(\theta) = 1/\sin\theta$, the resulting beampattern is the cylindrical hypercardioid.

C. Supercardioid

The supercardioid corresponds to the beampattern with maximum front-to-back ratio. Its coefficients can be derived from [5], [24]

$$\begin{aligned}\boldsymbol{\varrho}_{\mathrm{Sd}} &= \arg\max_{\boldsymbol{\varrho}} \frac{\int_0^{\pi/2} \mathcal{B}^2(\theta)\sin\theta d\theta}{\int_{\pi/2}^{\pi} \mathcal{B}^2(\theta)\sin\theta d\theta} \text{ s.t. } \boldsymbol{\varrho}^T\mathbf{x}(0) = 1 \\ &= \arg\max_{\boldsymbol{\varrho}} \frac{\boldsymbol{\varrho}^T\boldsymbol{\Upsilon}_{\mathrm{Sd,f}}\boldsymbol{\varrho}}{\boldsymbol{\varrho}^T\boldsymbol{\Upsilon}_{\mathrm{Sd,b}}\boldsymbol{\varrho}} \text{ s.t. } \boldsymbol{\varrho}^T\mathbf{x}(0) = 1,\end{aligned} \tag{38}$$

where $\boldsymbol{\Upsilon}_{\mathrm{Sd,f}}$ and $\boldsymbol{\Upsilon}_{\mathrm{Sd,b}}$ are two matrices of size $(Q+1) \times (Q+1)$, and whose (i, j)th elements are

$$[\boldsymbol{\Upsilon}_{\mathrm{Sd,f}}]_{i,j} = \int_0^1 x^{i+j-2}dx = \frac{1}{i+j-1} \tag{39}$$

and

$$[\boldsymbol{\Upsilon}_{\mathrm{Sd,b}}]_{i,j} = \int_{-1}^0 x^{i+j-2}dx = \frac{(-1)^{i+j}}{i+j-1}, \tag{40}$$

respectively. It can be deduced that

$$\boldsymbol{\varrho}_{\mathrm{Sd}} = \frac{1}{\mathbf{x}^T(0)\boldsymbol{\nu}_{\max}}\boldsymbol{\nu}_{\max}, \tag{41}$$

where $\boldsymbol{\nu}_{\max}$ is the eigenvector corresponding to the maximum eigenvalue of $\boldsymbol{\Upsilon}_{\mathrm{Sd,b}}^{-1}\boldsymbol{\Upsilon}_{\mathrm{Sd,f}}$.

Again, a more general case of the supercardioid can be derived from [24]

$$\max_{\boldsymbol{\varrho}} \frac{\int_0^{\theta_{\mathrm{TH}}} \psi(\theta)\mathcal{B}^2(\theta)\sin\theta d\theta}{\int_{\theta_{\mathrm{TH}}}^{\pi} \psi(\theta)\mathcal{B}^2(\theta)\sin\theta d\theta} \text{ s.t. } \boldsymbol{\varrho}^T\mathbf{x}(0) = 1, \tag{42}$$

where $\psi(\theta)$ is a proper weight function and $\theta_{\mathrm{TH}} \in (0,\pi)$ is a threshold parameter. By adding the constraint [25]:

$$\int_0^{\theta_{\mathrm{TH}}} \left|\frac{\partial\mathcal{B}(\theta)}{\partial\theta}\right|^2 d\theta \le \epsilon \tag{43}$$

into the optimization problem (42), where ϵ is a small positive number, one can also control the flatness of the beampattern in the interval $[0,\theta_{\mathrm{TH}}]$.

D. Chebyshev-Type

A Q th-order Chebyshev polynomial with respect to the variable z can be written as [5]

$$T_Q(z) = \begin{cases} \cos(Q\arccos z), & |z| \le 1 \\ \dfrac{\left(z-\sqrt{z^2-1}\right)^Q + \left(z+\sqrt{z^2-1}\right)^Q}{2}, & |z| > 1 \end{cases} \tag{44}$$

If we replace z with $a\cos\theta + b$, $T_Q(z)$ becomes a Q th-order polynomial with respect to $\cos\theta$.

The Chebyshev polynomial is a cosine function when $|z| \le 1$ and, at the same time, it is a monotonically increasing or decreasing function when $|z| > 1$. Therefore, as long as $|a\cos 0 + b| \ge 1$ and $|a\cos 180^\circ + b| \le |a\cos 0 + b|$, the base pattern:

$$\mathcal{B}(\theta) = \frac{1}{T_Q(a+b)} T_Q(a\cos\theta + b) \tag{45}$$

is always effective. The beampattern shape, the positions of the nulls, and the mainlobe-to-sidelobe ratio can all be controlled with the two parameters a and b.

Given the values of the parameters a and b, the nulls of the Chebyshev-type beampattern are

$$\theta_{0;q} = \arccos\left\{\frac{1}{a}\left[\cos\left(\frac{2q-1}{2Q}\pi\right) - b\right]\right\},\ q = 1,2,\ldots,Q. \tag{46}$$

Therefore, the first $Q+1$ coefficients of the beampattern can be deduced as

$$[\boldsymbol{\varrho}]_{1:Q+1} = \boldsymbol{\Gamma}^{-1}\mathbf{i}, \tag{47}$$

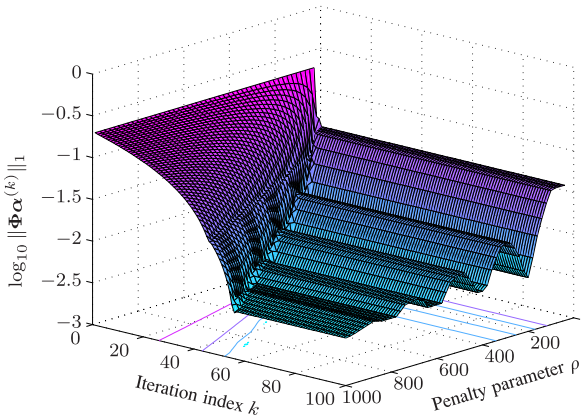

Fig. 3. $\log_{10}\|\boldsymbol{\Phi}\boldsymbol{\alpha}^{(k)}\|_1$, i.e., $\log_{10}\|\mathbf{X}^T\boldsymbol{\Psi}\boldsymbol{\alpha}^{(k)}\|_1$, as a function of the iteration index k with different values of the penalty parameter ρ.

where

$$\boldsymbol{\Gamma} = \begin{pmatrix} 1 & 1 & 1 & \cdots & 1 \\ 1 & \cos\theta_{0;1} & \cos^2\theta_{0;1} & \cdots & \cos^Q\theta_{0;1} \\ 1 & \cos\theta_{0;2} & \cos^2\theta_{0;2} & \cdots & \cos^Q\theta_{0;2} \\ \vdots & \vdots & \vdots & \ddots & \vdots \\ 1 & \cos\theta_{0;Q} & \cos^2\theta_{0;Q} & \cdots & \cos^Q\theta_{0;Q} \end{pmatrix} \tag{48}$$

is a Vandermonde matrix and $\mathbf{i} = [1\ \mathbf{0}^T]^T$ with $\mathbf{0}$ being a zero vector of length Q.

In case that the mainlobe width, θ_{MW} $[\theta_{\mathrm{MW}} \in (0,\pi)]$, is given, we can compute a and b according to

$$\begin{cases} a\cos\theta_{\mathrm{MW}} + b = 1 \\ a\cos\pi + b = -1 \\ a + b \ge 1 \end{cases}. \tag{49}$$

It is easy to deduce that

$$a = \frac{2}{1+\cos\theta_{\mathrm{MW}}}, \tag{50}$$

$$b = \frac{1-\cos\theta_{\mathrm{MW}}}{1+\cos\theta_{\mathrm{MW}}}, \tag{51}$$

and the sidelobe level (SLL) is

$$\mathrm{SLL} = 1/T_Q\left[\frac{3-\cos\theta_{\mathrm{MW}}}{1+\cos\theta_{\mathrm{MW}}}\right]. \tag{52}$$

If we want to reject signals coming from the range from θ_{RL} to θ_{RH}, we can calculate a and b according to

$$\begin{cases} a\cos\theta_{\mathrm{RL}} + b = 1 \\ a\cos\theta_{\mathrm{RH}} + b = -1 \\ a\cos 0 + b \ge 1 \\ a\cos\pi + b \le 0 \\ |a\cos\pi + b| \le |a\cos 0 + b| \end{cases}. \tag{53}$$

It can be deduced that

$$a = \frac{2}{\cos\theta_{\mathrm{RL}} - \cos\theta_{\mathrm{RH}}}, \tag{54}$$

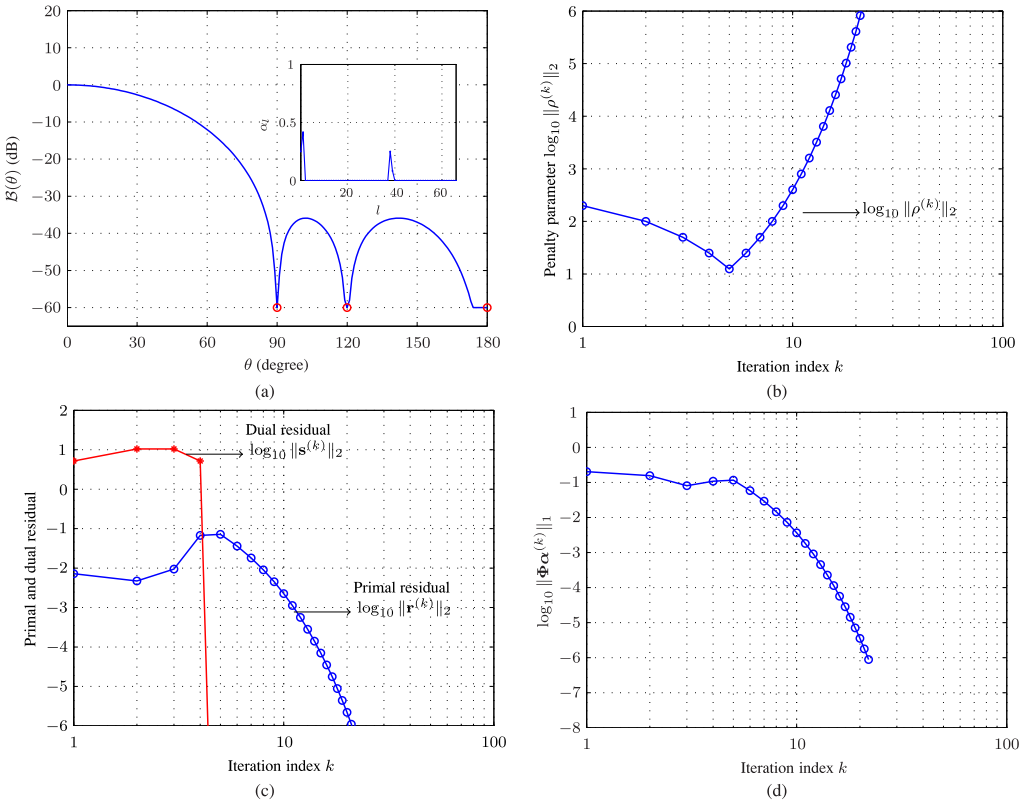

Fig. 4. An example of target beampatterns designed by the proposed approach using the ADMM algorithm, where the pattern order is $N = 3$, three nulls are at 90°, 120°, and 180°, $\epsilon^{\text{prim}} = \epsilon^{\text{dual}} = 10^{-6}$, and $\rho^0 = 200$. (a) Resulting beampattern and the associated α_l's; (b) varying the penalty parameter ρ with iteration index k; (c) primal and dual residuals with iteration index k; and (d) cost function $\log_{10}\|\mathbf{\Phi}\boldsymbol{\alpha}^{(k)}\|_1$.

$$b = -\frac{\cos\theta_{\text{RL}} + \cos\theta_{\text{RH}}}{\cos\theta_{\text{RL}} - \cos\theta_{\text{RH}}}, \tag{55}$$

$$0 \geq \cos\theta_{\text{RL}} + \cos\theta_{\text{RH}}, \tag{56}$$

and the sidelobe level is

$$\text{SLL} = 1/T_Q \left[\frac{2 - (\cos\theta_{\text{RL}} + \cos\theta_{\text{RH}})}{\cos\theta_{\text{RL}} - \cos\theta_{\text{RH}}}\right]. \tag{57}$$

E. Effective Combinations

Considering two base patterns $\mathcal{B}_1(\theta)$ and $\mathcal{B}_2(\theta)$, which satisfy the SE-condition, it is easy to verify that

$$\mathcal{B}(\theta) = \mathcal{B}_1(\theta)\mathcal{B}_2(\theta) \tag{58}$$

always satisfies the SE-condition, and the corresponding beampattern coefficients are the convolution of those of the two base patterns, i.e.,

$$\varrho_i = \sum_j \varrho_{1;j}\varrho_{2;i-j},\ i = 0, 1, \ldots, Q. \tag{59}$$

F. A Brief Summary

In the previous subsections, we have derived null-constrained base patterns including the dipole, cardioid, supercardioid, hypercardioid, and Chebyshev patterns with different mainlobe widths and sidelobe levels. It is shown that the combination of those aforementioned patterns are also effective DMA base patterns. Along with the monopole pattern, i.e., $\mathcal{B}(\theta) = 1$, one can construct more sets of base patterns by setting different values of the parameters of those aforementioned base patterns, e.g., the order, the nulls, the side-lobe level, etc.

Note that the first null (the null next to the look direction [29]) is often used to describe the mainlobe width. It should be pointed out that the smallest first null of a DMA is $\pi/(2N)$, i.e., $90^\circ/N$ (see Appendix A). Therefore, in practice, one should never expect an effective beampattern having a first null smaller than $90^\circ/N$.

V. Verification

The purpose of this section is to show how to design target beampatterns with the proposed method. The effectiveness of the resulting target beampattern is guaranteed by the positive superposition theorem, which does not need further justification. The organization of this section is as follows. In Section V-A, we show how to build a set of base patterns. In Section V-B, we verify the effectiveness of the ADMM algorithm to solve our optimization problem. In Section V-C, we present examples designed by the proposed method and compare those with the traditional ones. Finally, in Section V-D, we discuss how to further improve the performance of the proposed method.

A. Construction of a Set of Base Patterns

To design a DMA target beampattern of order N with the proposed approach, we need to first build a set of base patterns.

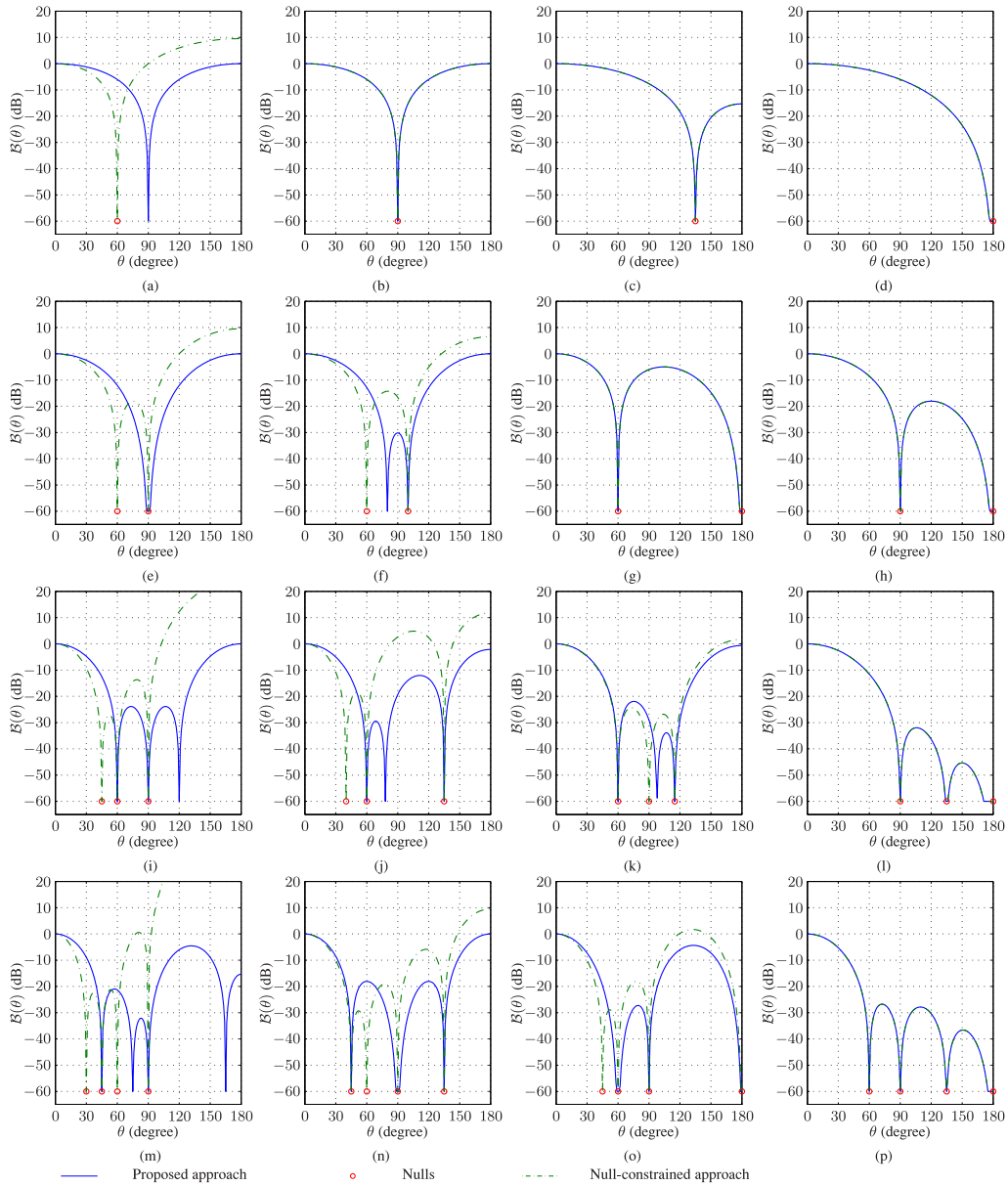

Fig. 5. Examples of the target beampatterns designed with the proposed approach, where (a)–(d) are for the first order beampatterns; (e)–(h) are for the second order beampatterns; (i)–(l) are for the third order beampatterns; (m)–(p) are for the fourth order beampatterns. The directions of desired nulls in the sub-figures are respectively: (a) 60°; (b) 90°; (c) 135°; (d) 180°; (e) $60^\circ, 90^\circ$; (f) $60^\circ, 100^\circ$; (g) $60^\circ, 180^\circ$; (h) $90^\circ, 180^\circ$; (i) $45^\circ, 60^\circ, 90^\circ$; (j) $40^\circ, 60^\circ, 135^\circ$; (k) $60^\circ, 90^\circ, 115^\circ$; (l) $90^\circ, 135^\circ, 180^\circ$; (m) $30^\circ, 45^\circ, 60^\circ, 90^\circ$; (n) $45^\circ, 60^\circ, 90^\circ, 135^\circ$; (o) $45^\circ, 60^\circ, 90^\circ, 180^\circ$; (p) $60^\circ, 90^\circ, 135^\circ, 180^\circ$.

In our examples, the base set consists of the following six classes of patterns.

- The first base pattern is the monopole, i.e., $\mathcal{B}_0(\theta) = 1$.
- The second class consists of the beampatterns with only one null (can be of multiplicity), where the coefficients are calculated according to (34) with $\zeta_1 = \cos(90^\circ + j10^\circ)$, $j = 0, 1, 2, \ldots, 9$, and the order $Q = 1, 2, \ldots, N$.
- The third class is the hypercardioid of different orders, where the coefficients are calculated according to (35) with the order $Q = 1, 2, \ldots, N$.
- The fourth class is the supercardioid of different orders, where the coefficients are calculated according to (41) with the order $Q = 1, 2, \ldots, N$.
- The fifth class is the Chebyshev-type beampattern with different mainlobe widths, where the coefficients are calculated according to (47) with the order $Q = 1, 2, \ldots, N$ and $\theta_{\mathrm{MW}} = 0^\circ, 30^\circ, 60^\circ, 90^\circ, 120^\circ, 150^\circ$.
- The sixth class is the Chebyshev-type beampattern under controlled rejection zones, where the coefficients are calculated according to (47) with the order $Q = 1, 2, \ldots, N$, $\theta_{\mathrm{RL}} = 30^\circ, 40^\circ, 50^\circ, 60^\circ$, and $\theta_{\mathrm{RH}} = \theta_{\mathrm{RL}} + 120^\circ$.

In total, the set of base patterns consists of $22N + 1$ patterns.

B. The ADMM Algorithm and an Example

According to (72), (73), and (74) in Appendix A, the value of the parameter ρ should be set before solving the optimization

problem in (27) by the ADMM algorithm. Figure 3 plots the values of $\log_{10}\|\mathbf{\Phi}\boldsymbol{\alpha}^{(k)}\|_1$ as a function of the parameter ρ and the iteration index k, where $N = 3$ and three nulls of the desired beampattern are at 90°, 120°, and 180°. As seen, we achieved better results with a larger value of ρ, while the convergence rate will be slower as the value of ρ increases. To reduce the sensitivity of the algorithm to the parameter ρ, we choose a varying penalty parameter according to (78); more details of which can be found in [26], [30], and [31]. Two parameters ϵ^{prim} and ϵ^{dual} are set to be 10^{-6} in the stopping criteria (75). The initial penalty parameter ρ is set to be $\rho^{(1)} = 200$.

A target beampattern design example is shown in Fig. 4. Figure 4(a) plots the designed target beampattern and the values of the associated α_l's with $N = 3$ and three nulls at 90°, 120°, and 180°. As one can see, this beampattern can be constructed with only four base patterns, and the gains in the nulls' directions are very close to zero according to the cost function in Fig. 4(d). Figure 4(c) plots the primal and dual residuals with the iteration index k and Fig. 4(b) plots the value of the varying penalty parameter ρ with the iteration index k. As seen, at the beginning, the dual residual is larger than 10 times of the primal one and the value of ρ decreases with iteration. After the first several iterations, the dual residual is very small.

C. Comparison With the Null-Constrained Design Method

In this subsection, we briefly compared the presented method with the null-constrained method, which is fundamental method to design target beampatterns. The corresponding beampatterns can be formed from (11) directly. Figure 5(d), (h), (l), and (p) plot the results with well-conditioned nulls, which shows that constraining the beampattern to form nulls in the desired directions will lead to effective beampatterns. Figure 5(a), (e), (i), and (m) plot the results with ill-conditioned nulls, where all the nulls are in $(0^\circ, 90^\circ)$. One can observe that those beampatterns are not effective. In comparison, all the beampatterns designed by the presented method are effective.

D. Validation on a Large Data Set and the Evolution of the Base-Pattern Set

In this subsection, the order of the target beampattern is set to $N = 4$. To test the performance of the proposed method, we generate one well-conditioned beampattern set with 10^5 samples, and one ill-conditioned beampattern set with 10^5 samples as well. The performance is then evaluated by showing the value of the beampattern at the direction of desired nulls.

- The results associated with the ill-conditioned set are shown in Fig. 6(b). It can be seen that the algorithm does yield nulls in most null directions.
- The results corresponding to the well-conditioned set are shown in Fig. 6(a). As seen, the presented approach successfully formed nulls in the nulls' directions most of the time; but, it failed for a small number of sets. The underlying reason may be that the number of patterns in the base set is not sufficiently large.

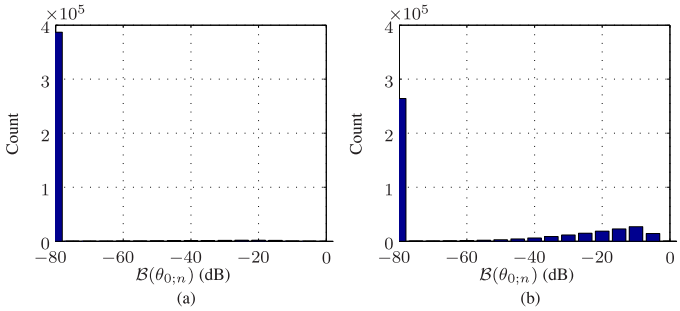

Fig. 6. The histogram of values at nulls' directions with primary base-pattern set. (a) Well-conditioned testing set. (b) Ill-conditioned testing set.

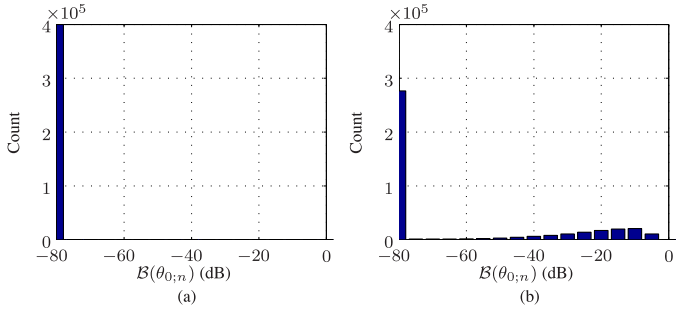

Fig. 7. The histogram of values at nulls' directions with expanded base-pattern set. (a) Well-conditioned testing set. (b) Ill-conditioned testing set.

To expand the base-pattern set, we generate another well-conditioned beampattern set with 10^5 samples; the set for expanding is not the same as the set for testing. The base-pattern set is expanded by the following two steps.

Step 1: Redesign the beampatterns with the proposed method, and check the value of $\sum_{n=1}^{N}|\mathcal{B}(\theta_{0;n})|$ for each beampattern. Pick up the beampattern corresponding to the maximum value.

Step 2: Add the beampattern to the base-pattern set. Go back to step 1.

After 154 iterations, the maximum value of $\sum_{n=1}^{N}|\mathcal{B}(\theta_{0;n})|$ is smaller than 10^{-3}; then, we end the iteration. The total number of the base patterns is now 243. With the new base-pattern set, the performance on the testing set is shown in Fig. 7. As seen, the number of failure cases remarkably decreased. So, in practice, one can reduce the failure cases by increasing the base set.

VI. Conclusions

The target beampattern of a DMA determines the array performance and how the array responds to the differential sound pressure field of different orders. A well-determined target beampattern can make the DMA perform better in terms of signal preservation and noise reduction. In this paper, we presented an approach to the design of target DMA beampatterns based on the nulls that we want to place in these target beampatterns. The major contribution consists of five aspects. First, we presented a

superposition theorem, which shows that the linear combination of any two effective base patterns with nonnegative coefficients is still an effective beampattern. Second, we formulated the target beampattern design problem into one of optimization, which can be solved by the well-known ADMM algorithm. Third, since the presented approach requires a set of effective base patterns, we derived many effective base beampatterns based on the use of some classical principles developed in the DMA literature. Fourth, we showed that the smallest first null of a DMA is $\pi/(2N)$ with N being the order of the DMA, which provides the rule of setting nulls in practice. Finally, by designing beampatterns with representative sets of nulls, we validated the feasibility of the presented approach to the design of effective and valid target beampatterns. The results demonstrated that the presented method is able to form effective beampatterns as long as the base set is sufficiently large.

Appendix A
Solving the Optimization Problem With the ADMM Algorithm

Defining $\mathbf{\Phi} = \mathbf{X}^T\mathbf{\Psi}$ and $\boldsymbol{\eta} = \mathbf{\Psi}^T\mathbf{x}(0)$, we can rewrite (27) as

$$\min_{\boldsymbol{\alpha}} \|\mathbf{\Phi}\boldsymbol{\alpha}\|_1 \ \text{ s.t. } \ \boldsymbol{\eta}^T\boldsymbol{\alpha} = 1 \\ \alpha_l \geq 0, \ \forall l = 0, 1, \ldots, L. \tag{60}$$

If we define a new vector $\mathbf{z} = \mathbf{\Phi}\boldsymbol{\alpha}$, (60) can be rewritten as

$$\min_{\boldsymbol{\alpha},\mathbf{z}} \|\mathbf{z}\|_1 \ \text{ s.t. } \ \mathbf{\Phi}\boldsymbol{\alpha} - \mathbf{z} = \mathbf{0} \\ \boldsymbol{\eta}^T\boldsymbol{\alpha} = 1 \\ \alpha_l \geq 0, \ \forall l = 0, 1, \ldots, L. \tag{61}$$

Now, if we take

$$\mathbf{A} = \begin{bmatrix} \boldsymbol{\eta}^T \\ \mathbf{\Phi} \end{bmatrix}, \ \mathbf{B} = \begin{bmatrix} \mathbf{0} \\ -\mathbf{I} \end{bmatrix}, \text{ and } \mathbf{c} = \begin{bmatrix} 1 \\ \mathbf{0} \end{bmatrix},$$

(61) can be further rewritten as

$$\min_{\boldsymbol{\alpha},\mathbf{z}} \|\mathbf{z}\|_1 \ \text{ s.t. } \ \mathbf{A}\boldsymbol{\alpha} + \mathbf{B}\mathbf{z} = \mathbf{c} \\ \alpha_l \geq 0, \ \forall l = 0, 1, \ldots, L. \tag{62}$$

As a result, the corresponding augmented Lagrangian is

$$\mathcal{L}_\rho(\boldsymbol{\alpha}, \mathbf{z}, \mathbf{y}) = \|\mathbf{z}\|_1 + \mathbf{y}^T(\mathbf{A}\boldsymbol{\alpha} + \mathbf{B}\mathbf{z} - \mathbf{c}) \\ + \frac{\rho}{2}\|\mathbf{A}\boldsymbol{\alpha} + \mathbf{B}\mathbf{z} - \mathbf{c}\|_2^2 \\ \text{s.t. } \alpha_l \geq 0, \ \forall l = 0, 1, \ldots, L. \tag{63}$$

It follows then that the ADMM iteration process is

$$\boldsymbol{\alpha}^{(k+1)} \leftarrow \arg\min_{\boldsymbol{\alpha}} \mathcal{L}_\rho\left[\boldsymbol{\alpha}, \mathbf{z}^{(k)}, \mathbf{y}^k\right], \\ \text{s.t. } \alpha_l \geq 0, \ \forall l = 0, 1, \ldots, L, \tag{64}$$

$$\mathbf{z}^{(k+1)} \leftarrow \arg\min_{\mathbf{z}} \mathcal{L}_\rho\left[\boldsymbol{\alpha}^{(k)}, \mathbf{z}, \mathbf{y}^k\right], \tag{65}$$

$$\mathbf{y}^{(k+1)} \leftarrow \mathbf{y}^{(k)} + \rho\left[\mathbf{A}\boldsymbol{\alpha}^{(k)} + \mathbf{B}\mathbf{z}^{(k)} - \mathbf{c}\right], \tag{66}$$

which can be further written as

$$\boldsymbol{\alpha}^{(k+1)} \leftarrow \arg\min_{\boldsymbol{\alpha}} \left\|\mathbf{A}\boldsymbol{\alpha} - \left[\mathbf{c} - \mathbf{B}\mathbf{z}^{(k)} - \frac{2}{\rho}\mathbf{y}^{(k)}\right]\right\|_2^2, \\ \text{s.t. } \alpha_l \geq 0, \ \forall l = 0, 1, \ldots, L, \tag{67}$$

$$\mathbf{z}^{(k+1)} \leftarrow \arg\min_{\mathbf{z}} \|z\|_1 + \frac{\rho}{2}\left\|\mathbf{z} - \left[\mathbf{\Phi}\boldsymbol{\alpha}^{(k)} - \frac{1}{\rho}\mathbf{B}^T\mathbf{y}^{(k)}\right]\right\|_2^2, \tag{68}$$

$$\mathbf{y}^{(k+1)} \leftarrow \mathbf{y}^{(k)} + \rho\left[\mathbf{A}\boldsymbol{\alpha}^{(k)} + \mathbf{B}\mathbf{z}^{(k)} - \mathbf{c}\right]. \tag{69}$$

The solution of the optimization problem in (68) has a closed form, i.e.,

$$\mathbf{z}^{(k+1)} \leftarrow S_{\frac{1}{\rho}}\left[\mathbf{\Phi}\boldsymbol{\alpha}^{(k)} - \frac{1}{\rho}\mathbf{B}^T\mathbf{y}^{(k)}\right], \tag{70}$$

where

$$S_\kappa(a) = (1 - \kappa/|a|)_+ a \tag{71}$$

is a soft thresholding operator.

Therefore, the iterative process from (67) to (69) can be further written as

$$\boldsymbol{\alpha}^{(k+1)} \leftarrow \arg\min_{\boldsymbol{\alpha}} \left\|\mathbf{A}\boldsymbol{\alpha} - \left[\mathbf{c} - \mathbf{B}\mathbf{z}^{(k)} - \frac{2}{\rho}\mathbf{y}^{(k)}\right]\right\|_2^2, \\ \text{s.t. } \alpha_l \geq 0, \ \forall l = 0, 1, \ldots, L, \tag{72}$$

$$\mathbf{z}^{(k+1)} \leftarrow S_{\frac{1}{\rho}}\left[\mathbf{\Phi}\boldsymbol{\alpha}^{(k)} - \frac{1}{\rho}\mathbf{B}^T\mathbf{y}^{(k)}\right], \tag{73}$$

$$\mathbf{y}^{(k+1)} \leftarrow \mathbf{y}^{(k)} + \rho\left[\mathbf{A}\boldsymbol{\alpha}^{(k)} + \mathbf{B}\mathbf{z}^{(k)} - \mathbf{c}\right], \tag{74}$$

where the optimization problem (67) can be solved with nonnegative least-squares (NNLS) algorithm derived in [32]. It is the *lsqnonneg* function in Matlab; more details of which can be found in [32].

Remark I: The iterative process stops if [26]

$$\|\mathbf{r}^{(k+1)}\|_2 \leq \epsilon^{\text{prim}} \text{ and } \|\mathbf{s}^{(k+1)}\|_2 \leq \epsilon^{\text{dual}}, \tag{75}$$

where

$$\mathbf{r}^{(k+1)} = \mathbf{A}\boldsymbol{\alpha}^{(k+1)} + \mathbf{B}\mathbf{z}^{(k+1)} - \mathbf{c}, \tag{76}$$

$$\mathbf{s}^{(k+1)} = \rho\mathbf{A}^T\mathbf{B}\left[\mathbf{z}^{(k+1)} - \mathbf{z}^{(k)}\right], \tag{77}$$

are the primal and dual residuals, respectively.

Remark II: An effective and efficient scheme for varying the penalty parameter ρ is [26], [30], [31]

$$\rho^{(k+1)} = \begin{cases} 2\rho^{(k)}, & \text{if } \|\mathbf{r}^{(k)}\|_2 \geq 10\|\mathbf{s}^{(k)}\|_2 \\ \frac{1}{2}\rho^{(k)}, & \text{if } \|\mathbf{s}^{(k)}\|_2 \geq 10\|\mathbf{r}^{(k)}\|_2 \\ \rho^{(k)}, & \text{otherwise} \end{cases}. \tag{78}$$

The algorithm is summarized in Algorithm 1.

Appendix B
The Smallest First Null of DMAs

The first null of a beampattern is defined as the null closest to the look direction. In this section, we derive the smallest first null

Algorithm 1: Solve (27) by ADMM Algorithm.

$[\boldsymbol{\alpha}, \boldsymbol{\Psi}] = \text{optimal\_pattern\_nulls}(N, \{\theta_{0;n}\})$
· Calculate $\boldsymbol{\Psi}$ according to Section IV
· Calculate $\mathbf{X}$ and $\mathbf{x}(0)$ according to (28) and (20)
· Calculate $\boldsymbol{\Phi}$, $\boldsymbol{\eta}$, $\mathbf{A}$, $\mathbf{B}$ and $\mathbf{c}$ according to Appendix A
· Set $\rho^{(0)} = 200$, $\epsilon^{\text{prim}} = \epsilon^{\text{dual}} = 10^{-6}$
· Set $\boldsymbol{\alpha}^{(0)} = [1\ 1\ \cdots\ 1]^T/(L+1)$
· Set $\mathbf{z}^{(0)} = \boldsymbol{\Phi}\boldsymbol{\alpha}^{(0)}$
· Set $\mathbf{y}^{(0)} = \rho^{(0)}\left[\mathbf{A}\boldsymbol{\alpha}^{(0)} + \mathbf{B}\mathbf{z}^{(0)} - \mathbf{c}\right]$
· For k = 1, 2, 3,...
  · $\rho = \rho^{(k-1)}$;
  · Calculate $\boldsymbol{\alpha}^{(k)}$ according to (72)
  · Calculate $\mathbf{z}^{(k)}$ according to (73) and (71)
  · Calculate $\mathbf{y}^{(k)}$ according to (74)
  · Calculate $\mathbf{r}^{(k)}$ and $\mathbf{s}^{(k)}$ according to (76) and (77)
  · If $\|\mathbf{r}^{(k)}\|_2 \le \epsilon^{\text{prim}}$ and $\|\mathbf{s}^{(k)}\|_2 \le \epsilon^{\text{dual}}$
    · $\boldsymbol{\alpha} = \boldsymbol{\alpha}^{(k)}$
    · Return $\boldsymbol{\alpha}$ and $\boldsymbol{\Psi}$
  · End
  · Calculate $\rho^{(k)}$ according to (78)
· End

of a DMA beampattern, which can provide the rule for setting nulls in practice.

Let's define the nulls as $\theta_{0;1} \le \theta_{0;2} \le \cdots \le \theta_{0;N}$. Assuming that we have an initial $\mathcal{B}(\theta)$, the maximum value of the $|\mathcal{B}(\theta)|$ in the interval of $[\theta_{0;1}, \pi]$ is equal to 1, and the $\mathcal{B}(\theta)$ in this interval is not equi-ripple. According to the alternation theorem [33], by changing the nulls $\theta_{0;2}, \ldots, \theta_{0;N}$, we can have an equi-ripple beampattern in which the absolute value of the extrema is smaller than 1. Based on this derivation, the beampattern that has the smallest first null satisfies the following two properties.

1) The maximum absolute value of the extrema is equal to 1. Otherwise, we can always have a smaller first null.
2) The beampattern in the interval of $[\theta_{0;1}, \pi]$ is equi-ripple. Otherwise, we can always have an equi-ripple beampattern whose absolute value of the extrema is smaller than 1, and further we can have a smaller first null.

By considering that the value of the beampattern at $\theta = 0$ is equal to 1, i.e., equal to the absolute value of the extrema, $\mathcal{B}(0)$ can be viewed as an extrema if we take $[0, \pi]$ as the interval. Therefore, the beampattern that has the smallest first nulls is the solution of the following minimax optimization problem:

$$\min t \text{ s.t. } |\mathcal{B}(\theta)| \le t,\ \forall \theta \in [0, \pi]$$
$$\mathcal{B}(0) = 1. \tag{79}$$

The solution is an equi-ripple beampattern and the absolute value of the extrema is equal to 1.

Since $\mathcal{B}(\theta)$ is an Nth order polynomial with respect to $\cos\theta$, the maximum number of nulls we have in the interval of $[0, \pi]$ is N. Therefore, the number of the extrema in the interval of $(0, \pi)$ is $N-1$. By considering the two extrema at $\theta = 0$ and $\theta = \pi$, the solution of (79) has $N+1$ extrema in total.

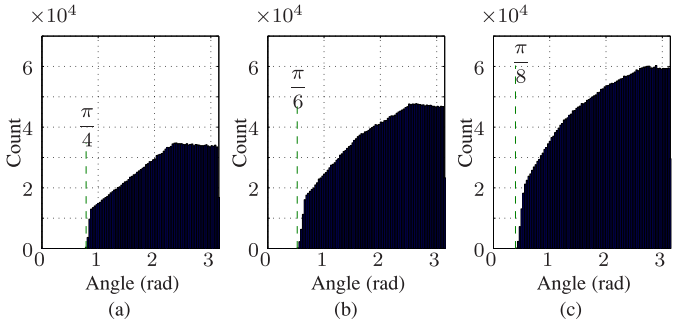

Fig. 8. The histogram of the nulls with 1 million random beampatterns that are effective: (a) $N = 2$, (b) $N = 3$, and (c) $N = 4$.

It can be verified that the Nth order polynomial $\cos(N\theta)$ has $N+1$ extrema in the interval of $[0, \pi]$, which are $\theta_k = k\pi/N, k = 0, 1, \ldots, N$. At the same time, it is an equi-ripple beampattern, and the absolute value of the extrema is equal to 1. Therefore, $\cos(N\theta)$ is the solution of (79). Since (79) is a convex optimization problem, $\cos(N\theta)$ is the only solution. Therefore, it is safe to say that $\cos(N\theta)$ is the beampattern having the smallest first null. The corresponding first null is $\pi/(2N)$.

To further verify this limitation, we randomly generate 1 million effective beampatterns. The histogram of the nulls are shown in Fig. 8. As we can see, no nulls smaller than $\pi/(2N)$ can be formed in the effective beampatterns.

REFERENCES

[1] H. F. Olson, "Gradient microphones," *J. Acoust. Soc. Am.*, vol. 17, pp. 192–198, Jan. 1946.
[2] J. Benesty and J. Chen, *Study and Design of Differential Microphone Arrays*. Berlin, Germany: Springer-Verlag, 2012.
[3] G. W. Elko and J. Meyer, "Microphone arrays," in *Springer Handbook of Speech Processing*, J. Benesty, M. M. Sondhi, and Y. Huang, Eds. Berlin, Germany: Springer-Verlag, 2008, ch. 50, pp. 1021–1041.
[4] G. W. Elko and A.-T. N. Pong, "A simple adaptive first-order differential microphone," in *Proc. IEEE Workshop Appl. Signal Process. Audio Acoust.*, 1995, pp. 169–172.
[5] G. W. Elko, "Differential microphone arrays," in *Audio Signal Processing: For Next-Generation Multimedia Communication Systems*, Y. Huang and J. Benesty, Eds. Boston, MA, USA: Springer-Verlag, 2004, ch. 2, pp. 11–65.
[6] J. Chen, J. Benesty, and C. Pan, "On the design and implementation of linear differential microphone arrays," *J. Acoust. Soc. Am.*, vol. 136, pp. 3097–3113, Dec. 2014.
[7] C. Pan, J. Chen, and J. Benesty, "Theoretical analysis of differential microphone array beamforming and an improved solution," *IEEE/ACM Trans. Audio, Speech, Lang. Process.*, vol. 23, no. 11, pp. 2093–2105, Nov. 2015.
[8] L. Zhao, J. Benesty, and J. Chen, "Design of robust differential microphone arrays," *IEEE/ACM Trans. Audio, Speech, Lang. Process.*, vol. 22, no. 10, pp. 1455–1466, Oct. 2014.
[9] C. Pan, J. Benesty, and J. Chen, "Design of robust differential microphone arrays with orthogonal polynomials," *J. Acoust. Soc. Am.*, vol. 138, no. 2, pp. 1079–1089, Aug. 2015.
[10] G. Huang, J. Benesty, and J. Chen, "On the design of frequency-invariant beampatterns with uniform circular microphone arrays," *IEEE/ACM Trans. Audio, Speech, Lang. Process.*, vol. 25, no. 5, pp. 1140–1153, May 2017.

[11] C. P. Mathews and M. D. Zoltowski, "Eigenstructure techniques for 2-D angle estimation with uniform circular arrays," *IEEE Trans. Signal Process.*, vol. 42, no. 9, pp. 2395–2407, Sep. 1994.
[12] J. Meyer, "Beamforming for a circular microphone array mounted on spherically shaped objects," *J. Acoust. Soc. Am.*, vol. 109, pp. 185–193, Jan. 2001.
[13] B. Rafaely, "Analysis and design of spherical microphone arrays," *IEEE Trans. Audio, Speech, Lang. Process.*, vol. 13, no. 1, pp. 135–143, Jan. 2005.
[14] S. C. Chan and H. H. Chen, "Uniform concentric circular arrays with frequency-invariant characteristics–Theory, design, adaptive beamforming and DOA estimation," *IEEE Trans. Signal Process.*, vol. 55, no. 1, pp. 165–177, Jan. 2007.
[15] S. Yan, H. Sun, X. Ma, U. P. Svensson, and C. Hou, "Time-domain implementation of broadband beamformer in spherical harmonics domain," *IEEE Trans. Audio, Speech, Lang. Process.*, vol. 19, no. 5, pp. 1221–1230, Jul. 2011.
[16] S. Yan, "Optimal design of modal beamformers for circular arrays," *J. Acoust. Soc. Am.*, vol. 138, no. 4, pp. 2140–2151, 2015.
[17] B. Rafaely, *Fundamentals of Spherical Array Processing*. Berlin, Germany: Springer, 2015.
[18] J. Benesty, M. Souden, and Y. Huang, "A perspective on differential microphone arrays in the context of noise reduction," *IEEE Trans. Audio, Speech, Lang. Process.*, vol. 20, no. 2, pp. 699–704, Feb. 2012.
[19] M. Buck, "Aspects of first-order differential microphone arrays in the presence of sensor imperfections," *Eur. Trans. Telecommun.*, vol. 13, pp. 115–122, Mar./Apr. 2002.
[20] J. Benesty, J. Chen, and I. Cohen, *Design of Circular Differential Microphone Arrays*. Basel, Switzerland: Springer-Verlag, 2015.
[21] H. Zhang, J. Chen, and J. Benesty, "Study of nonuniform linear differential microphone arrays with the minimum-norm filter," *Appl. Acoust.*, vol. 98, pp. 62–69, Nov. 2015.
[22] Y. Buchris, I. Cohen, and J. Benesty, "Frequency-domain design of asymmetric circular differential microphone arrays," *IEEE/ACM Trans. Audio, Speech, Lang. Process.*, vol. 26, no. 4, pp. 760–773, May 2018.
[23] C. Pan, J. Benesty, and J. Chen, "Design of directivity patterns with a unique null of maximum multiplicity," *IEEE/ACM Trans. Audio, Speech, Lang. Process.*, vol. 24, no. 2, pp. 226–235, Feb. 2016.
[24] J. Benesty, J. Chen, and C. Pan, *Fundamentals of Differential Beamforming* Springer Briefs in Electrical and Computer Engineering. New York, NY, USA: Springer, 2016.
[25] E. De Sena, H. Hacihabiboglu, and Z. Cvetkovic, "On the design and implementation of higher-order differential microphones," *IEEE Trans. Audio, Speech, Lang. Process.*, vol. 20, no. 1, pp. 162–174, Jan. 2012.
[26] S. Boyd, N. Parikh, E. Chu, B. Peleato, and J. Eckstein, "Distributed optimization and statistical learning via the alternating direction method of multipliers," *Found. Trends Mach. Learn.*, vol. 3, no. 1, pp. 1–122, 2010.
[27] M. Elad, *Sparse and Redundant Representations: From Theory to Applications in Signal and Image*. New York, NY, USA: Springer-Verlag, 2010.
[28] M. Grant, S. Boyd, and Y. Ye, "CVX: Matlab software for disciplined convex programming, version 1.21 (2011)," 2010, [Online]. Available: *cvxr. com/cvx*
[29] H. L. Van Trees, *Optimum Array Processing: Part IV of Detection, Estimation, and Modulation*. New York, NY, USA: Wiley, 2004.
[30] B. S. He, H. Yang, and S. L. Wang, "Alternating direction method with self-adaptive penalty parameters for monotone variational inequalities," *J. Optim. Theory. Appl.*, vol. 106, pp. 337–356, Aug. 2000.
[31] S. L. Wang and L. Z. Liao, "Decomposition method with a variable parameter for a class of monotone variational inequality problems," *J. Optim. Theory. Appl.*, vol. 109, no. 2, pp. 415–429, 2001.
[32] C. L. Lawson and R. J. Hanson, *Solving Least Squares Problems*. Upper Saddle River, NJ, USA: Prentice-Hall, 1974, pp. 160–161.
[33] T. Parks and J. Mcclellan, "Chebyshev approximation for nonrecursive digital filters with linear phase," *IEEE Trans. Circuit Theory*, vol. 19, no. 2, pp. 189–194, Mar. 1972.

Chao Pan was born in 1989. He received the Bachelor's degree in electronics and information engineering and the Ph.D. degree in information and communication engineering from the Northwestern Polytechnical University, Xian, China, in 2011 and 2018, respectively.

From November 2014 to November 2016, he was a visiting Ph.D. student with the University of Quebec, INRS-EMT, Montreal, QC, Canada. He is currently a Lecturer with the School of Artificial Intelligence, Xidian University. His research interests include acoustic signal processing, array signal processing, differential microphone array, sound field measuring and reproduction, signal separation, speech enhancement, brain science, and deep learning.

Dr. Pan received the IEEE Region 10 (Asia-Pacific) 2016 Distinguished Student Paper Award (First Prize) (with Chen and Benesty) for his journal paper *Theoretical Analysis of Differential Microphone Array Beamforming and an Improved Solution*. As a Reviewer, he serves the IEEE TRANSACTIONS ON AUDIO, SPEECH, AND LANGUAGE PROCESSING, the IEEE SIGNAL PROCESSING LETTER, and several international conferences.

Jingdong Chen (M'99–SM'09) received the Ph.D. degree in pattern recognition and intelligence control from the Chinese Academy of Sciences, Beijing, China, in 1998.

From 1998 to 1999, he was with ATR Interpreting Telecommunications Research Laboratories, Kyoto, Japan, where he conducted research on speech synthesis, speech analysis, as well as objective measurements for evaluating speech synthesis. He then joined the Griffith University, Brisbane, Australia, where he engaged in research on robust speech recognition and signal processing. From 2000 to 2001, he worked at ATR Spoken Language Translation Research Laboratories on robust speech recognition and speech enhancement. From 2001 to 2009, he was a Member of Technical Staff with Bell Laboratories, Murray Hill, NJ, USA, working on acoustic signal processing for telecommunications. He subsequently joined WeVoice Inc., Bridgewater Township, NJ, USA, serving as the Chief Scientist. He is currently a Professor with the Northwestern Polytechnical University, Xi'an, China. He coauthored the books *Design of Circular Differential Microphone Arrays* (Springer, 2015), *Study and Design of Differential Microphone Arrays* (Springer, 2013), *Speech Enhancement in the STFT Domain* (Springer, 2011), *Optimal Time-Domain Noise Reduction Filters: A Theoretical Study* (Springer, 2011), *Speech Enhancement in the Karhunen-Loève Expansion Domain* (Morgan & Claypool, 2011), *Noise Reduction in Speech Processing* (Springer, 2009), *Microphone Array Signal Processing* (Springer, 2008), and *Acoustic MIMO Signal Processing* (Springer, 2006). His research interests include acoustic signal processing, adaptive signal processing, speech enhancement, adaptive noise/echo control, microphone array signal processing, signal separation, and speech communication.

Dr. Chen served as an Associate Editor of the IEEE TRANSACTIONS ON AUDIO, SPEECH, AND LANGUAGE PROCESSING from 2008 to 2014. He is currently a Technical Committee (TC) member of the IEEE Signal Processing Society TC on Audio and Electroacoustics, and a Member of the editorial advisory board of the *Open Signal Processing Journal*. He was the Technical Program Chair of IEEE TENCON 2013, a Technical Program Co-Chair of IEEE WASPAA 2009, IEEE ChinaSIP 2014, IEEE ICSPCC 2014, and IEEE ICSPCC 2015, and helped organize many other conferences.

He received the 2008 Best Paper Award from the IEEE Signal Processing Society (with Benesty, Huang, and Doclo), the best paper award from the IEEE Workshop on Applications of Signal Processing to Audio and Acoustics (WASPAA) in 2011 (with Benesty), the Bell Labs Role Model Teamwork Award twice, respectively, in 2009 and 2007, the NASA Tech Brief Award twice, respectively, in 2010 and 2009, the Young Author Best Paper Award from the fifth National Conference on Man-Machine Speech Communications in 1998. He was also a recipient of the Japan Trust International Research Grant from the Japan Key Technology Center in 1998 and the "Distinguished Young Scientists Fund" from the National Natural Science Foundation of China in 2014.

Jacob Benesty received the Master's degree in microwaves from Pierre & Marie Curie University, Paris, France, in 1987, and the Ph.D. degree in control and signal processing from Orsay University, Orsay, France, in April 1991. During his Ph.D. (from November 1989 to April 1991), he worked on adaptive filters and fast algorithms with the Centre National d'Etudes des Telecommunications, Paris, France. From January 1994 to July 1995, he was with Telecom Paris University on multichannel adaptive filters and acoustic echo cancelation. From October 1995 to May 2003, he was first a Consultant and then a Member of the Technical Staff with Bell Laboratories, Murray Hill, NJ, USA. In May 2003, he joined the University of Quebec, INRS-EMT, Montreal, Quebec, Canada, as a Professor. He is also a Visiting Professor with the Technion, Haifa, Israel, an Adjunct Professor with Aalborg University, Aalborg, Denmark, and a Guest Professor with Northwestern Polytechnical University, Xi'an, Shaanxi, China.

His research interests include signal processing, acoustic signal processing, and multimedia communications. He is the inventor of many important technologies. In particular, he was the Lead Researcher with Bell Labs who conceived and designed the world-first real-time hands-free full-duplex stereophonic teleconferencing system. Also, he conceived and designed the world-first PC-based multiparty hands-free full-duplex stereo conferencing system over IP networks.

He is the Editor of the book series *Springer Topics in Signal Processing*. He was the General Chair and Technical Chair of many international conferences and a Member of several IEEE technical committees. Four of his journal papers were awarded by the IEEE Signal processing Society and, in 2010, he received the Gheorghe Cartianu Award from the Romanian Academy. He has coauthored and coedited/coauthored numerous books in the area of acoustic signal processing.

Guangming Shi (SM'10) received the B.S. degree in automatic control, the M.S. degree in computer control, and the Ph.D. degree in electronic information technology from Xidian University, Xi'an, China, in 1985, 1988, and 2002, respectively.

In 1988, he joined the School of Electronic Engineering, Xidian University. From 1994 to 1996, he was a Research Assistant with the Department of Electronic Engineering, University of Hong Kong. In 2004, he had studied with the Department of Electronic Engineering, University of Illinois at Urban–Champaign. Since 2003, he has been a Professor with the Xidian University. He is currently the Academic Leader on circuits and systems, and the Chair Professor with the School of Artificial Intelligence, Xidian University. His research interests include compressed sensing, image processing, computer vision, and brain-inspired computing. He has authored or coauthored more than 300 research papers and several books in the related areas. In 2012, he was awarded the "Cheung Kong (Changjiang) Scholar Chair Professor" from the Chinese Ministry of Education.